

---

# SYNTHETIC DATA FROM DIFFUSION MODELS IMPROVES DRUG DISCOVERY PREDICTION

---

**Bing Hu**

Computer Science  
University of Waterloo  
bingxu.hu@uwaterloo.ca

**Ashish Saragadam**

School of Public Health Sciences  
University of Waterloo  
asaragadam@uwaterloo.ca

**Anita Layton**

Applied Mathematics  
University of Waterloo  
anita.layton@uwaterloo.ca

**Helen Chen**

School of Public Health Sciences  
University of Waterloo  
helen.chen@uwaterloo.ca

## ABSTRACT

Artificial intelligence (AI) is increasingly used in every stage of drug development. Continuing breakthroughs in AI-based methods for drug discovery require the creation, improvement, and refinement of drug discovery data. We posit a new data challenge that slows the advancement of drug discovery AI: datasets are often collected independently from each other, often with little overlap, creating data sparsity. Data sparsity makes data curation difficult for researchers looking to answer key research questions requiring values posed across multiple datasets. We propose a novel diffusion GNN model Syngand capable of generating ligand and pharmacokinetic data end-to-end. We show and provide a methodology for sampling pharmacokinetic data for existing ligands using our Syngand model. We show the initial promising results on the efficacy of the Syngand-generated synthetic target property data on downstream regression tasks with AqSolDB, LD50, and hERG central. Using our proposed model and methodology, researchers can easily generate synthetic ligand data to help them explore research questions that require data spanning multiple datasets.

**Keywords** Synthetic Data · Diffusion Models · Drug Discovery · AI

## 1 Introduction

There is a growing trend towards leveraging artificial intelligence (AI) in every stage of drug development [1]. Drug development is an expensive process: it costs \$2-3 billion dollars and 13-15 years to bring a single drug to market. Drug discovery AI, by enabling the high-throughput screening (HTS) of ligand candidates, is geared to reduce the developmental costs of drugs by revolutionizing how ligands are designed and tested [2]. Drug development AI has found great initial success such as in poly-pharmacy [3], drug re-purposing [4, 5], drug-target interaction [6], drug response prediction [7], and in search of new antibiotics [8]. Equally important to advances in AI for drug discovery are the equal improvements in available public data for training and testing these models [9, 10, 11].

Only through equal strides in the development and refinement of drug discovery data, and the application of advanced AI models to that data, do breakthroughs happen for AI-based methods for drug discovery. Huang et al. [9] noted 3 key challenges for drug discovery data to attracting ML scientists to therapeutics: (1) a lack of AI-ready datasets and standardized knowledge representations; (2) datasets scattered around the bio-repositories without curation; (3) a lack of data focused for rare diseases and novel drugs in development. We posit another data challenge that slows the advancement of drug discovery AI: datasets are often collected independently, often with little overlap, creating data sparsity. Data sparsity poses difficulties for researchers looking to answer research questions requiring data values posed across multiple different datasets.

Although there are advances towards large-scale data repositories containing vast broad data about each ligand [11, 12] and cells [13, 9], these large-scale data repositories face unique challenges for scalability and data sparsity. Auxiliary data often needs to be gathered for each ligand, such as on pharmacokinetic values of water solubility [14], toxicity [15], and hERG [16]. However, as data repositories become larger, that task becomes increasingly expensive and time-consuming. In this paper, we propose Syngand, an end-to-end generative AI diffusion model, that can solve both problems of data sparsity and scalability faced by data repositories. Our model is trained to generate novel ligands with synthetic pharmacokinetic data that describe them or fill in pharmacokinetic data when given an existing ligand.

Recent advances combining Denoising diffusion probabilistic models (DDPMs) [17] with graph-neural networks (GNNs) have resulted in a new class of diffusion models capable of generating ligand structures [18, 19, 20, 21]. Although some use ligand properties to aid in the conditional generation of the ligand [22], none aim to generate pharmacokinetic data alongside the ligand diffusion pipeline. A recent study in diffusion-generated synthetic data [23] has shown improvements in performance for ImageNet classification with synthetic augmented real image data. In the present study, we show that diffusion-generated synthetic ligand data can be used to improve performance on downstream drug discovery regression tasks for water solubility [14], acute toxicity (LD50) [15], and hERG Central [16].

Our contributions are as follows:

- We propose a novel diffusion GNN model Syngand capable of generating ligand and pharmacokinetic data end-to-end.
- We develop a methodology for sampling pharmacokinetic data for existing ligands using our model.
- We show promising initial results for the efficacy of the generated synthetic data in augmenting real data for downstream pharmacokinetic tasks for AqSolDB [14], LD50 Toxicity [15], and hERG Central [16].

## 2 Background

Diffusion methods model complex datasets using families of probability distribution while maintaining computational tractability for learning, sampling, inference and evaluation [18]. The denoising diffusion probabilistic model (DDPMs) approach [17] systematically destroys the structure in the data through a forward diffusion process, and then in a reverse diffusion process, learns how to restore the structure in the data from noise. DDPMs have been increasingly used for drug discovery to allow for the rapid generation and high throughput screening (HTS) of drug candidates [24, 25].

Conditional Diffusion models based on discrete Graph Structures (CDGS) can be used to generate small-molecule molecular graphs with similar distributions to real small-molecules [22]. The CDGS method utilizes a graph noise prediction model built using hybrid message passing blocks (HMPB) [22], which allows for aggregation of local and global node and edge features. CDGS differs from [26] which uses separate networks for node and edge denoising. E(n)-equivariant GNN (EGNN) [27] introduces a new model capable of learning graph equivariant to rotations, translations, and permutations. The EGNN architecture is the basis of E(3)-equivariant diffusion model (EDM) [28] that performs a diffusion process in euclidean space to generate small-molecules. An alternative approach based on EGNN is DiffBridge [20] which uses Lyapunov functions to create prior bridges, injecting physical and statistics information, to guide the diffusion process. Compared to EGNN [27] and EDM [28], DiffBridge showed improved performance in terms of physical energy and molecular stability during molecule generation [20]. Digress [19] combines discrete diffusion [29] and graph transformers [30] for small-molecule generation. Digress utilizes a noise model *close to the true data distribution* [19] that preserves the marginal distribution of nodes and edge types rather than using uniform noise.

In conditional diffusion models [31, 32], an additional input is available during training and sampling which allows the model to generate data given the conditioning signal. Conditional guidance is utilized in Digress [19] on graph-level properties, such as cycles, and spectral and molecular features, to augment the input with auxiliary conditioning signals to improve training and sampling performance. Conditional guidance with target properties such as water solubility, binding affinity, toxicity, drug-likeness, and molecular weight is possible with latent state optimization or Monte-Carlo sampling to optimize molecule generation [33, 34, 35, 36]. Other works use reinforcement learning to generate molecules with specified properties such as weight or solubility [37, 38]. The challenge with these approaches is the generalizability of available datasets for these properties to the small-molecule search space. Datasets for important target properties such water solubility [14], LD50 toxicity [15], and hERG central [16] range between 7k-300k examples, which all pale in comparison to the combinatorial search space of all small-molecules.

Therapeutics Data Commons [9], PubChem [12], ZINC [39], ChEMBL and associated curations [11, 10] all aim to provide large data repositories of high-quality ligand data curated for drug discovery. Given the costly nature of data collection for drugs, extending additional pharmacokinetic properties across all ligands in a large data repository is expensive. Data sparsity is actuated by the expensive nature of data collection as only small sets of ligands can be

feasibly tested for target property data collection studies. Thus, the data sparsity challenge gives rise to barriers for researchers interested in answering key research questions requiring data across multiple datasets.

Determining the relationship between water solubility, toxicity, and ligand structure is an important research question for drug design [40, 41]. There are little over 300 ligands that can be collected from public datasets AqSolDB [14], LD50 toxicity [15], and hERG central [16] for researchers to look to analyze these complex relationships. As 300 ligands may not sufficiently generalize, additional data collection would be necessary.

In the present study, we aim to solve the data sparsity problem in drug discovery by training a model capable of generating synthetic ligand data. Our model Syngand extends existing ligand diffusion models by integrating target property generation with ligand generation in a fully end-to-end diffusion pipeline. As researchers may want to generate target properties for a fixed set of ligands, we provide a diffusion sampling method that can be used to generate target pharmacokinetic data when given an existing ligand. Finally, we show in initial experiments the efficacy of the generated synthetic data in augmenting real data for downstream drug-discovery regression tasks on AqSolDB [14], LD50 [15], and hERG central [16].

### 3 Methodology

The model is trained on 1.3 million ligands collected from Guacamol [10], and training property datasets AqSolDB [14], LD50 toxicity [15], and hERG Central [16]. Training property datasets are all collected from Therapeutics Data Commons (TDC) [9]. We selected a subset of 60k ligands from AqSolDB, LD50, and hERG Central to generate synthetic target properties for existing ligands.

#### 3.1 Data Processing

Guacamol contains around 1.27 million ligands curated from ChEMBL after charge neutralization, and removing salts, molecules with SMILES longer than 100 characters, molecules containing certain elements, and certain molecules for benchmark testing.

The target properties that we will be focusing on are AqSolDB [14], LD50 [15], and hERG Central [16]. AqSolDB [14] measures the aqueous solubility of around 9.9k ligands. Poor water solubility can lead to inadequate bioavailability and can be toxic. LD50 [15] measures the acute toxicity of around 7.3k ligands. hERG Central [16] measures the blocking of the human ether-a-go-go related gene (hERG) for around 306k ligands. hERG is crucial for coordinating the beating heart and we use values of hERG inhibition at  $1\mu\text{M}$  of the ligand. We will look to generate synthetic values for these 3 target properties through an end-to-end diffusion and sampling process. To train our Syngand diffusion network, we first have to construct a training dataset combining data from Guacamol [10] and our 3 target property datasets AqSolDB [14], LD50 [15], and hERG Central [16].

In merging the Guacamol dataset [10] with our target property datasets, we first identify common molecules between Guacamol and each target property dataset. As a percentage of each target property dataset, 32.4% of molecules in AqSolDB exist in Guacamol, 38.7% of molecules in LD50 exist in Guacamol, and 59.1% of hERG Central exist in Guacamol. After identifying common molecules between Guacamol and each target property dataset, we merge Guacamol and target property datasets AqSolDB, LD50, and hERG on these common molecules. Analyzing the merged dataset, of the 1.27 million ligands in Guacamol, 86.6% of these molecules do not have any target property values.

To improve the amount and quality of our training data, we look to add molecules in our target property datasets AqSolDB, LD50, and hERG Central that did not previously exist in Guacamol into our training data. As Guacamol contains molecules after careful curation from ChEMBL [10, 11], we follow similar filtering rules when adding molecules from target property datasets into our training data. We filter out any molecules from target property datasets that have molecule SMILES strings longer than 100 and molecules with elements besides the 13 included in Guacamol [10]. There are 1.33 million molecules in the training dataset after adding the filtered list of target property molecules, of which 82.7% of these molecules do not have any target properties.

#### 3.2 Syngand Model

We extend upon the base DiGress model [19] to create the novel Syngand model that is capable of end-to-end training and diffusion of target property values with ligand diffusion. We accomplish this by introducing an additional continuous diffusion process alongside the DiGress discrete diffusion process for the target properties. The same graph transformer network is used for Syngand as defined in DiGress. In this section, we focus on the formulation and algorithms for target property diffusion as described below.

### 3.2.1 Diffusion Process for Target Properties

Consider target properties  $\mathbf{y}$ . The diffusion process adds Gaussian noise independently to each target property:

$$q(\mathbf{y}^t | \mathbf{y}^{t-1}) = \mathcal{N}(\alpha^{t|t-1} \mathbf{y}^{t-1}, (\sigma^{t|t-1})^2 \mathbf{I}) \quad (1)$$

This process can be written as:

$$q(\mathbf{y}^t | \mathbf{y}) = \mathcal{N}(\mathbf{y}^t | \alpha^t \mathbf{y}, \sigma^t \mathbf{I}) \quad (2)$$

where  $\alpha^{t|t-1} = \alpha^t / \alpha^{t-1}$  and  $(\sigma^{t|t-1})^2 = (\sigma^t)^2 - (\alpha^{t|t-1})^2 (\sigma^{t-1})^2$ . To obtain a variance-preserving process, the variance chosen is  $(\sigma^t)^2 = 1 - (\alpha^t)^2$  [42]. The true denoising process can be computed in closed form:

$$q(\mathbf{y}^{t-1} | \mathbf{y}, \mathbf{y}^t) = \mathcal{N}(\mu^{t \leftarrow t-1}(\mathbf{y}, \mathbf{y}^t), (\sigma^{t \leftarrow t-1})^2 \mathbf{I}) \quad (3)$$

with

$$\mu^{t \leftarrow t-1}(\mathbf{y}, \mathbf{y}^t) = \frac{\alpha_{t|t-1} (\sigma^{t-1})^2}{\sigma_t^2} \mathbf{y}^t + \frac{\alpha^{t-1} (\sigma^{t|t-1})^2}{(\sigma^t)^2} \mathbf{y} \quad \text{and} \quad \sigma^{t \leftarrow t-1} = \frac{\sigma_{t|t-1} \sigma_{t-1}}{\sigma_t} \quad (4)$$

The denoising network is trained to predict the noise components  $\hat{\epsilon}_{\mathbf{y}}$  instead of  $\hat{\mathbf{y}}$  itself [17]. The equation is as follows:

$$\alpha^t \hat{\mathbf{y}} = \mathbf{y}^t - \sigma^t \hat{\epsilon}_{\mathbf{y}} \quad (5)$$

The network is optimized by minimizing the mean squared error between the predicted noise and true noise. Sampling is done similarly to standard Gaussian diffusion models.

### 3.3 Generation of Target Properties for Existing Ligands

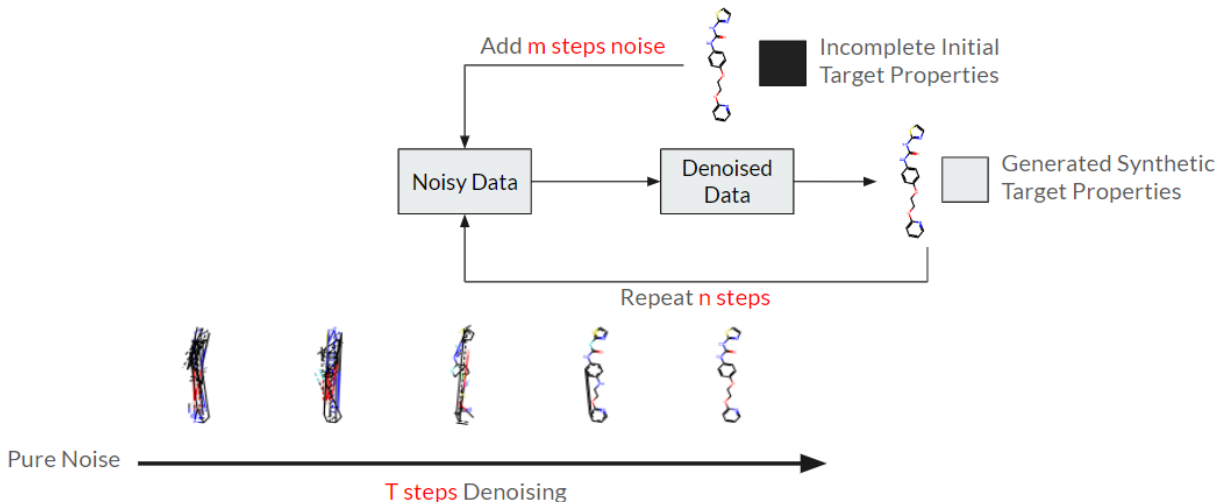


Figure 1: Overview of the methodology for generating target properties for existing ligands. Existing ligands with incomplected initial target properties are repeatedly partially denoised and the generated synthetic target properties are output.

We propose a novel generation process to generate target properties for existing ligands (Figure 1). This allows the Syngand model to both be able to generate target property values given an input ligand, as well as to generate new ligands and their target property values. This allows researchers flexibility to directly query target properties from the model for any number of ligands of interest quickly and efficiently.

Algorithm 1 shows the pseudocode for the proposed method to generate target properties for existing ligands. This methodology is similar to existing prior bridging techniques as used in DiffBridge [20]. The idea is to repeat a partial denoising process, while bridging in the desired ligand and any initial target property values, until a fixed number of repetitions is reached. The key parameters are the number of steps  $N$  in the denoising process and the number of times  $M$  this process is repeated. If no existing target properties exist for the input ligand graph  $G$ , the initial target properties  $\mathbf{y}$  can be imputed to average values. Likewise, if the input ligand has pre-existing target properties, the initial target properties  $\mathbf{y}$  can be initialized accordingly.

Algorithm 1: Generation of target properties for existing ligand

---

**Input:** A graph  $G = (\mathbf{X}, \mathbf{E})$ , initial target properties  $\mathbf{y}$ ,  $M$  iterations,  $N$  steps where  $N < T$

**for**  $it = M$  **to** 1 **do**

Sample  $G^N \sim \mathbf{X}\bar{\mathbf{Q}}_X^N \times E\bar{\mathbf{Q}}_E^N$  ▷ Sample a discrete noisy graph

Sample  $\epsilon_y \sim \mathcal{N}(0, \mathbf{I}_n)$  ▷ Sample a Gaussian noise for target properties

$z_y^N \leftarrow \alpha^N(\mathbf{y}) + \sigma_N(\epsilon_y)$

**for**  $t = N$  **to** 1 **do**

Sample  $\epsilon_y \sim \mathcal{N}(0, \mathbf{I}_n)$

$z \leftarrow f(G^t, t)$  ▷ Structural and spectral features as defined in DiGress

$\hat{p}^X, \hat{p}^E \leftarrow \phi_\theta(G^t, z)$  ▷ Forward Pass

$p_\theta(x_i^{t-1}|G^t) \leftarrow \sum_x q(x_i^{t-1}|x_i = x, x_i^t)\hat{p}_i^X(x)$  ▷ Posterior

$p_\theta(e_{ij}^{t-1}|G^t) \leftarrow \sum_e q(x_{ij}^{t-1}|e_{ij} = e, e_{ij}^t)\hat{p}_{ij}^X(e)$  ▷ Posterior

$G^{t-1} \sim \prod_i p_\theta(x_i^{t-1}|G^t) \prod_{i,j} p_\theta(e_{ij}^{t-1}|G^t)$  ▷ Categorical distr.

$z_y^{t-1} \leftarrow \frac{1}{\alpha_{t|t-1}}z^t - \frac{\sigma_{t|t-1}^2}{\alpha_{t|t-1}\sigma^t}\phi_\theta(z^t, t) + \sigma_{t \leftarrow t-1}(\epsilon_y)$  ▷ Reverse iteration for  $\mathbf{y}$

**end for**

$\mathbf{y} \leftarrow z_y^0$

**end for**

**return**  $\mathbf{y}$

---

## 4 Results

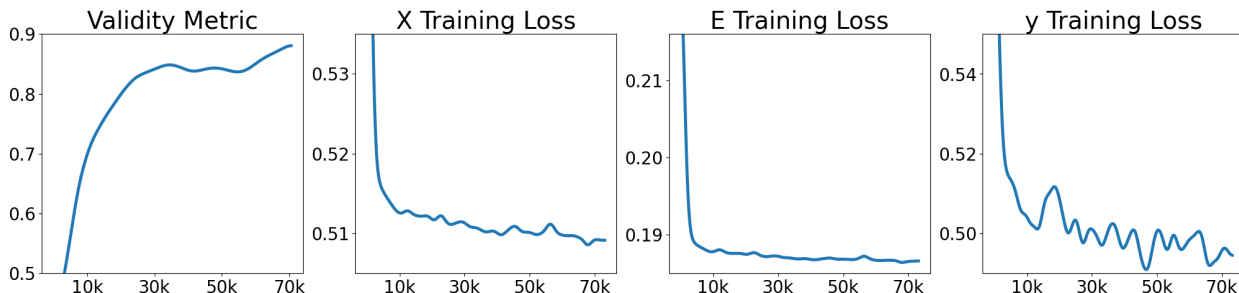


Figure 2: Pre-training loss for ligand graph  $G = (X, E)$  and  $\mathbf{y}$  target properties as well as the relaxed validity metric.

Figure 2 shows the pre-training graphs for the Syngand model. The model is trained for 100 epochs and validated after every epoch. The model is trained until convergence with vertex loss around 0.51, edge loss around 0.18, target property loss around 0.49, and validity around 88%. Relaxed validity is computed using RdKit [43] over 64 generated synthetic ligands. The pre-trained model is used for our experiment on generating synthetic target property values for select input ligands using Algorithm 1.

### 4.1 Generated Synthetic Target Properties

A set of 60k ligands are selected from AqSolDB [14], LD50 [15], and hERG Central [16]. The pre-trained model and algorithm Algorithm 1 is then applied to the selected ligands to generate synthetic target property values. We utilize parameters of  $N = 50$  (iterations) and  $M = 10$  (steps) for Algorithm 1. The generated synthetic dataset, containing 60k ligands with AqSolDB, LD50, and hERG values, can be used to augment real data in research work needing large quantities of ligands with data spanning these three datasets.

Figure 3 shows the distribution of the generated synthetic target properties for a set of 60k selected input ligands. Hellinger distances, 0.43, 0.50, and 0.08, are computed to compare the distribution of synthetically generated target properties with real target properties for AqSolDB, LD50, and hERG respectively.

Table 1 compares the mean and variance of the real and synthetically generated target property values. The mean of the generated synthetic data aligns closely with real data means with deviations between 2-16%. Synthetic data has variance much different from real data differing by a factor of 1.17-3.16x. The mean and variation of generated

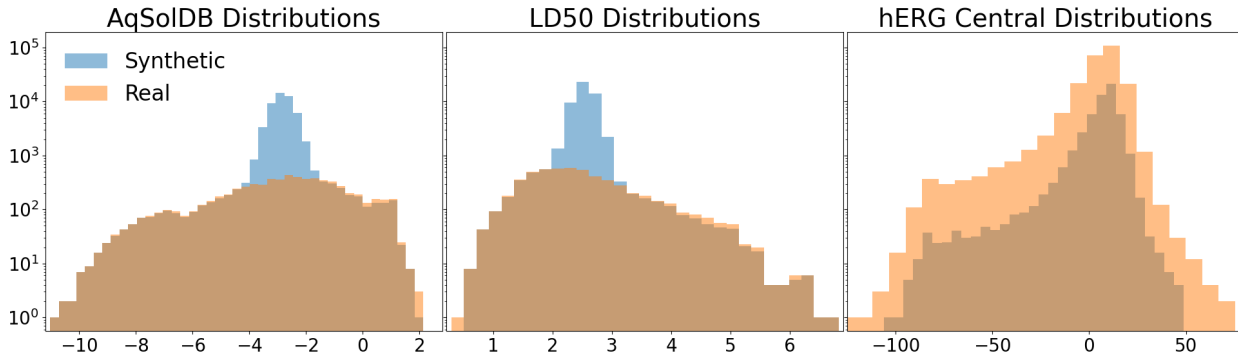


Figure 3: Distribution of generated synthetic target properties, AqSolDB (left), LD50 (middle), and hERG (right) for selected ligands. Synthetic distributions are in blue while real distributions are in yellow. Log scale is used for the y-axis.

Data	Real Mean (STD)	Synthetic Mean (STD)
AqSolDB	-2.91 (2.30)	-2.85 (0.87)
LD50	2.53 (0.95)	2.53 (0.30)
hERG	6.23 (11.18)	7.22 (9.55)

Table 1: Comparing mean and variance values between real and synthetic target property values.

synthetic data are affected by the noise sampling strategy, in our case Gaussian, and sampling hyperparameters of the number of iterations ( $M = 50$ ) and steps ( $M = 10$ ).

A key limitation is that the generated data remains clustered around the mean. Future work will look to optimize the noise sampling strategy and sampling hyperparameters to improve the univariate quality of the generated synthetic data compared to the real data. Additional pairwise correlations and multivariate statistical analysis will be conducted in future work to further evaluate the quality of the generated synthetic data.

## 4.2 Downstream Drug Discovery Regression Tasks

After the generation of synthetic target properties for our selected ligands, the quality of the generated target properties is measured by the performance of the synthetic data on a downstream task. In this experiment, we aim to measure the machine learning efficiency (MLE) [44] of the generated synthetic data. Machine learning efficiency (MLE) represents the ability of the generated data to replace or augment real data in the training process. MLE evaluates the performance of discriminative models trained on synthetic data. To measure MLE, the models are tested on real test data, and the scores are compared to the original performance when models are trained on real data [44].

For this experiment, we develop a Linear Regression (LR) and XGBoost (XGB) model for AqSolDB [14], LD50 [15], and hERG central [16] to evaluate our generated synthetic augmented real data for downstream drug discovery tasks. The model takes as input learned embeddings from ChemBERTa [45] of ligand SMILES to predict desired target property values using the discriminative models.

To prevent data leakage, we follow a procedure to first divide real and synthetic data before combining them to form train and test sets. We divide synthetic data into segments denoted  $A_s$  and  $B_s$  using a 85%/15% split. We divide real data into segments denoted  $A_r$  and  $B_r$  using a 50%/50% split. The real train set is defined as  $A_r$  and the real test set is defined as  $B_r$ . The augmented train set is defined as  $A_r \cup A_s$  and the augmented test set is defined as  $B_r \cup B_s$ . Outliers are removed from both real and augmented train and test sets based on  $\pm 1.5$ IQR bounds on the synthetic data.

Table 2 shows the results of downstream task performance of using a synthetic augmented real dataset compared to just the real dataset. With our simple model, we show that an augmented dataset can outperform real data with statistical significance over 30 runs after removing outlier values. Additional models and downstream tasks will be explored in future work.

Data	Metric	Trainset-Testset		
		Aug-Aug	Aug-Real	Real-Real
AqSolDB	MSE	0.172	<b>0.399</b>	0.927
	MAE	0.329	<b>0.632</b>	0.753
	R2	0.018	<b>0.053</b>	-1.199
	PCC	0.149	<b>0.263</b>	0.19
LD50	MSE	0.029	<b>0.072</b>	0.345
	MAE	0.135	<b>0.226</b>	0.459
	R2	0.075	<b>0.017</b>	-2.292
	PCC	0.279	<b>0.151</b>	0.094
hERG	MSE	29.8	<b>34.0</b>	34.7
	MAE	4.32	<b>4.76</b>	4.81
	R2	0.01	<b>0.002</b>	-0.018
	PCC	0.129	<b>0.102</b>	0.098

Table 2: Comparing drug discovery regression performances between different combinations of augmented and real train sets, and augmented and real test sets. Values are averaged over 30 trials with the best scores on the real test set bolded. The underlined values are statistically significant. Hyphenated pairs correspond to the train and test set used in the experiment.

## 5 Conclusion

In this paper, we developed Syngand, an end-to-end model and methodology that can generate novel ligands and their corresponding target properties. Additionally, we propose a novel method for generating target property values given an existing ligand using our Syngand model. Finally, we show the efficacy of the generated synthetic ligand data by comparing performance on downstream drug discovery regression tasks with AqSolDB, LD50, and hERG. One key limitation of this work is the poor univariate quality of the synthetic data being too clustered compared to the real data. Further hyperparameter optimizations will need to be explored to improve on the quality of the generated synthetic data. Other limitations are to expand the scope of the research to also measure the multivariate quality of the generated synthetic data, and to expand downstream testing of the synthetic data to include additional tasks and models. Although there are key limitations that still need to be addressed, our methods show promise in tackling the data sparsity problem in drug discovery.

Future work will look to improve our methods, scale to additional target properties, generate more synthetic data and create better evaluations of this new class of synthetic data. A crucial direction for this research is to improve the quality of the generated synthetic data to extend our results to more complex downstream tasks and models. Additional ablation and configuration studies will be explored in future work. Drug discovery researchers can immediately benefit from Syngand given how easily and quickly they can generate data they need to investigate previously infeasible research questions that span multiple datasets. Through addressing data sparsity in drug discovery, our methods work to accelerate drug discovery research and drug discovery AI.

## References

- [1] Jintae Kim, Sera Park, Dongbo Min, and Wankyu Kim. Comprehensive survey of recent drug discovery using deep learning. *International Journal of Molecular Sciences*, 22(18):9983, 2021.
- [2] Sudeep Pushpakom, Francesco Iorio, Patrick A Eyers, K Jane Escott, Shirley Hopper, Andrew Wells, Andrew Doig, Tim Guilleams, Joanna Latimer, Christine McNamee, et al. Drug repurposing: progress, challenges and recommendations. *Nature reviews Drug discovery*, 18(1):41–58, 2019.
- [3] Marinka Žitnik, Edward A Nam, Christopher Dinh, Adam Kuspa, Gad Shaulsky, and Blaž Zupan. Gene prioritization by compressive data fusion and chaining. *PLoS computational biology*, 11(10):e1004552, 2015.
- [4] Maha A Thafar, Mona Alshahrani, Somayah Albaradei, Takashi Gojobori, Magbubah Essack, and Xin Gao. Affinity2vec: drug-target binding affinity prediction through representation learning, graph mining, and machine learning. *Scientific reports*, 12(1):4751, 2022.
- [5] Deisy Morselli Gysi, Ítalo do Valle, Marinka Zitnik, Asher Ameli, Xiao Gan, Onur Varol, Susan Dina Ghiassian, J. J. Patten, Robert A. Davey, Joseph Loscalzo, and Albert-László Barabási. Network medicine framework for identifying drug-repurposing opportunities for covid-19. *Proceedings of the National Academy of Sciences*, 118(19), April 2021.

- [6] Majun Lian, Wenli Du, Xinjie Wang, and Qian Yao. Drug-target interaction prediction based on multi-similarity fusion and sparse dual-graph regularized matrix factorization. *IEEE Access*, 9:99718–99730, 2021.
- [7] Maryam Pouryahya, Jung Hun Oh, James C Mathews, Zehor Belkhatir, Caroline Moosmüller, Joseph O Deasy, and Allen R Tannenbaum. Pan-cancer prediction of cell-line drug sensitivity using network-based methods. *International Journal of Molecular Sciences*, 23(3):1074, 2022.
- [8] Jonathan M Stokes, Kevin Yang, Kyle Swanson, Wengong Jin, Andres Cubillos-Ruiz, Nina M Donghia, Craig R MacNair, Shawn French, Lindsey A Carfrae, Zohar Bloom-Ackermann, et al. A deep learning approach to antibiotic discovery. *Cell*, 180(4):688–702, 2020.
- [9] Kexin Huang, Tianfan Fu, Wenhao Gao, Yue Zhao, Yusuf Roohani, Jure Leskovec, Connor W. Coley, Cao Xiao, Jimeng Sun, and Marinka Zitnik. Therapeutics data commons: Machine learning datasets and tasks for drug discovery and development, 2021.
- [10] Nathan Brown, Marco Fiscato, Marwin H.S. Segler, and Alain C. Vaucher. Guacamol: Benchmarking models for de novo molecular design. *Journal of Chemical Information and Modeling*, 59(3):1096–1108, 2019. PMID: 30887799.
- [11] Anna Gaulton, Anne Hersey, Michał Nowotka, A Patricia Bento, Jon Chambers, David Mendez, Prudence Mutowo, Francis Atkinson, Louisa J Bellis, Elena Cibrián-Uhalte, et al. The chembl database in 2017. *Nucleic acids research*, 45(D1):D945–D954, 2017.
- [12] Sunghwan Kim, Jie Chen, Tiejun Cheng, Asta Gindulyte, Jia He, Siqian He, Qingliang Li, Benjamin A Shoemaker, Paul A Thiessen, Bo Yu, et al. Pubchem 2023 update. *Nucleic acids research*, 51(D1):D1373–D1380, 2023.
- [13] Xin Jin, Zelalem Demere, Karthik Nair, Ahmed Ali, Gino B Ferraro, Ted Natoli, Amy Deik, Lia Petronio, Andrew A Tang, Cong Zhu, et al. A metastasis map of human cancer cell lines. *Nature*, 588(7837):331–336, 2020.
- [14] Murat Cihan Sorkun, Abhishek Khetan, and Süleyman Er. Aqsolddb, a curated reference set of aqueous solubility and 2d descriptors for a diverse set of compounds. *Scientific data*, 6(1):143, 2019.
- [15] Hao Zhu, Todd M Martin, Lin Ye, Alexander Sedykh, Douglas M Young, and Alexander Tropsha. Quantitative structure- activity relationship modeling of rat acute toxicity by oral exposure. *Chemical research in toxicology*, 22(12):1913–1921, 2009.
- [16] Fang Du, Haibo Yu, Beiyang Zou, Joseph Babcock, Shunyou Long, and Min Li. hergcentral: a large database to store, retrieve, and analyze compound-human ether-a-go-go related gene channel interactions to facilitate cardiotoxicity assessment in drug development. *Assay and drug development technologies*, 9(6):580–588, 2011.
- [17] Jonathan Ho, Ajay Jain, and Pieter Abbeel. Denoising diffusion probabilistic models, 2020.
- [18] Zhiye Guo, Jian Liu, Yanli Wang, Mengrui Chen, Duolin Wang, Dong Xu, and Jianlin Cheng. Diffusion models in bioinformatics and computational biology. *Nature Reviews Bioengineering*, pages 1–19, 2023.
- [19] Clement Vignac, Igor Krawczuk, Antoine Siraudin, Bohan Wang, Volkan Cevher, and Pascal Frossard. Digress: Discrete denoising diffusion for graph generation, 2023.
- [20] Lemeng Wu, Chengyue Gong, Xingchao Liu, Mao Ye, and Qiang Liu. Diffusion-based molecule generation with informative prior bridges, 2022.
- [21] Ilia Igashov, Hannes Stärk, Clément Vignac, Victor Garcia Satorras, Pascal Frossard, Max Welling, Michael Bronstein, and Bruno Correia. Equivariant 3d-conditional diffusion models for molecular linker design, 2022.
- [22] Han Huang, Leilei Sun, Bowen Du, and Weifeng Lv. Conditional diffusion based on discrete graph structures for molecular graph generation, 2023.
- [23] Shekoofeh Azizi, Simon Kornblith, Chitwan Saharia, Mohammad Norouzi, and David J Fleet. Synthetic data from diffusion models improves imagenet classification. *arXiv preprint arXiv:2304.08466*, 2023.
- [24] Rafael Gómez-Bombarelli, Jennifer N Wei, David Duvenaud, José Miguel Hernández-Lobato, Benjamín Sánchez-Lengeling, Dennis Sheberla, Jorge Aguilera-Iparraguirre, Timothy D Hirzel, Ryan P Adams, and Alán Aspuru-Guzik. Automatic chemical design using a data-driven continuous representation of molecules. *ACS central science*, 4(2):268–276, 2018.
- [25] Nicola De Cao and Thomas Kipf. Molgan: An implicit generative model for small molecular graphs. *arXiv preprint arXiv:1805.11973*, 2018.
- [26] Jaehyeong Jo, Seul Lee, and Sung Ju Hwang. Score-based generative modeling of graphs via the system of stochastic differential equations, 2022.
- [27] Victor Garcia Satorras, Emiel Hoogeboom, Fabian B. Fuchs, Ingmar Posner, and Max Welling. E(n) equivariant normalizing flows for molecule generation in 3d. *CoRR*, abs/2105.09016, 2021.



- [28] Emiel Hooeboom, Victor Garcia Satorras, Clément Vignac, and Max Welling. Equivariant diffusion for molecule generation in 3d, 2022.
- [29] Jacob Austin, Daniel D Johnson, Jonathan Ho, Daniel Tarlow, and Rianne Van Den Berg. Structured denoising diffusion models in discrete state-spaces. *Advances in Neural Information Processing Systems*, 34:17981–17993, 2021.
- [30] Vijay Prakash Dwivedi and Xavier Bresson. A generalization of transformer networks to graphs. *arXiv preprint arXiv:2012.09699*, 2020.
- [31] Chitwan Saharia, William Chan, Saurabh Saxena, Lala Li, Jay Whang, Emily Denton, Seyed Kamyar Seyed Ghasemipour, Burcu Karagol Ayan, S. Sara Mahdavi, Rapha Gontijo Lopes, Tim Salimans, Jonathan Ho, David J Fleet, and Mohammad Norouzi. Photorealistic text-to-image diffusion models with deep language understanding, 2022.
- [32] Aditya Ramesh, Prafulla Dhariwal, Alex Nichol, Casey Chu, and Mark Chen. Hierarchical text-conditional image generation with clip latents, 2022.
- [33] Ryan J Richards and Austen M Groener. Conditional beta-vae for de novo molecular generation. *arXiv preprint arXiv:2205.01592*, 2022.
- [34] Tristan Aumentado-Armstrong. Latent molecular optimization for targeted therapeutic design. *arXiv preprint arXiv:1809.02032*, 2018.
- [35] Seul Lee, Jaehyeong Jo, and Sung Ju Hwang. Exploring chemical space with score-based out-of-distribution generation. In *International Conference on Machine Learning*, pages 18872–18892. PMLR, 2023.
- [36] Mingyang Wang, Chang-Yu Hsieh, Jake Wang, Dong Wang, Gaoqi Weng, Chao Shen, Xiaojun Yao, Zhitong Bing, Honglin Li, Dongsheng Cao, et al. Relation: A deep generative model for structure-based de novo drug design. *Journal of Medicinal Chemistry*, 65(13):9478–9492, 2022.
- [37] Omar Mahmood, Elman Mansimov, Richard Bonneau, and Kyunghyun Cho. Masked graph modeling for molecule generation. *Nature communications*, 12(1):3156, 2021.
- [38] Youngchun Kwon, Jiho Yoo, Youn-Suk Choi, Won-Joon Son, Dongseon Lee, and Seokho Kang. Efficient learning of non-autoregressive graph variational autoencoders for molecular graph generation. *Journal of Cheminformatics*, 11, 11 2019.
- [39] John J Irwin and Brian K Shoichet. Zinc- a free database of commercially available compounds for virtual screening. *Journal of chemical information and modeling*, 45(1):177–182, 2005.
- [40] Yohei Kawabata, Koichi Wada, Manabu Nakatani, Shizuo Yamada, and Satomi Onoue. Formulation design for poorly water-soluble drugs based on biopharmaceutics classification system: Basic approaches and practical applications. *International Journal of Pharmaceutics*, 420(1):1–10, 2011.
- [41] Dixit V. Bhalani, Bhingaradiya Nutan, Avinash Kumar, and Arvind K. Singh Chandel. Bioavailability enhancement techniques for poorly aqueous soluble drugs and therapeutics. *Biomedicines*, 10(9), 2022.
- [42] Diederik P. Kingma, Tim Salimans, Ben Poole, and Jonathan Ho. Variational diffusion models, 2023.
- [43] Greg Landrum. Rdkit documentation. *Release*, 1(1-79):4, 2013.
- [44] Vadim Borisov, Kathrin Seßler, Tobias Leemann, Martin Pawelczyk, and Gjergji Kasneci. Language models are realistic tabular data generators. *arXiv preprint arXiv:2210.06280*, 2022.
- [45] Seyone Chithrananda, Gabriel Grand, and Bharath Ramsundar. Chemberta: Large-scale self-supervised pretraining for molecular property prediction, 2020.